International Journal of Pharmaceutics 679 (2025) 125751

Contents lists available at ScienceDirect

International Journal of Pharmaceutics

journal homepage: www.elsevier.com/locate/ijpharm

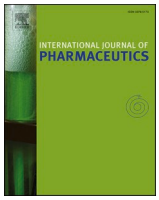

Review

Combining innovation and sustainable development in the 3D printing manufacturing of drug delivery and testing devices

Costanza Fratini [a,1], Ye Zhang [b,1], Sofia Moroni [a], Mattia Tiboni [a], Hui Xin Ong [c,d], Paul M. Young [c,d], Luca Casettari [a,*], Daniela Traini [c,d,*]

[a] Department of Biomolecular Sciences, University of Urbino Carlo Bo, Urbino, PU, Italy
[b] School of Life Sciences, Faculty of Science, University of Technology Sydney, NSW 2007, Australia
[c] Respiratory Technology, Woolcock Institute of Medical Research, NSW 2113, Australia
[d] Macquarie Medical School, Faculty of Medicine, Health and Human Sciences, Macquarie University, NSW 2113, Australia

ARTICLE INFO

Keywords:
3D printing
Additive manufacturing
Dose dispensing devices
in vitro drug testing models

ABSTRACT

Additive manufacturing (AM), commonly referred to as 3D printing (3DP), has made a significant impact on both manufacturing and healthcare, revolutionizing these industries. The key advantage of 3DP lies in rapid prototyping, which accelerates product development and iteration while reducing costs. This technology offers unmatched customization, particularly in the medical field, where it enables the creation of personalized treatments tailored to individual patients. In manufacturing, 3DP reduces material waste, promoting sustainability, while enhancing production efficiency by simplifying assembly processes and reducing supply chain complexity. Additionally, the decentralized nature of 3DP fosters creativity and accessibility, allowing individuals and businesses to innovate at a local level.

This review highlights the wide-ranging applications of 3DP in pharmaceutical and biomedical fields, from device prototyping to developing quality control systems for medical testing. As 3DP continues to evolve, it holds the potential to transform traditional manufacturing models, improving product quality, environmental impact, and cost-effectiveness. This progression supports the dual goals of more efficient, cost-effective production and patient-centric healthcare optimization.

1. Introduction

Additive manufacturing (AM), commonly referred to as 3D printing (3DP), is a method used to develop a three-dimensional object in a layer-by-layer manner. Although 3DP comprises different techniques such as fused deposition modelling (FDM), direct powder extrusion (DPE), semisolid extrusion (SSE), stereolithography (SLA), digital light processing (DLP), selective laser sintering (SLS), vat polymerisation and binder jetting, it consists of into two fundamental steps: computer-aided design (CAD) and object slicing. While 3DP initially emerged for rapid prototyping, advancements in accessible materials, speed, accuracy, and precision have made this process applicable to large-scale manufacturing. Particularly, in the pharmaceutical field it can be employed to meet patient-centric demands and overcome the *one-size-fits-all* criterion (Chen et al., 2020). Due to its potential for low-cost and customisable production of small batches, 3DP has gained significant attention in drug delivery and testing systems, with research in this area expanding rapidly in recent years. Personalization, on-demand manufacture, and product complexity are some of the primary benefits of additive manufacturing in pharmaceutical applications. Specifically, 3DP has been used not only to create novel and complex drug delivery systems that account for inter-individual variations in drug responses (Lim et al., 2018), but also to build models and tools that optimize medication based on each patient's unique characteristics. This review highlights studies that employ 3DP to manufacture devices for drug development and testing.

2. 3D-printed devices for continuous manufacturing

Due to its ability to transition quickly from concept to prototype at a reasonable cost, 3DP is becoming increasingly popular in the development of manufacturing devices. This is particularly true in the

* Corresponding authors.
E-mail address: luca.casettari@uniurb.it (L. Casettari).
[1] Authors contributed equivalently.

https://doi.org/10.1016/j.ijpharm.2025.125751
Received 14 March 2025; Received in revised form 16 May 2025; Accepted 20 May 2025
Available online 21 May 2025

pharmaceutical industry, where it reduces production expenses, minimizes material waste, and accelerate the development of new equipment. Furthermore, 3DP can produce intricate geometries that are challenging to achieve with other methods, making it an important tool for optimizing production technologies and enhancing product quality (Hirschberg et al., 2018a).

2.1. Powder mixing setups

Svane et al. (Svane et al., 2021) demonstrated the feasibility of using 3DP for rapid prototyping of tools that could be integrated into a continuous manufacturing (CM) line, by developing a model of miniaturized powder mixing geometries using Fused Deposition Modelling (FDM) with polylactic acid (PLA) and polyvinyl alcohol (PVA) (Fig. 1-A). Powder mixing, a critical step in pharmaceutical production, is typically performed in batches. However, in CM lines, continuous powder mixing is essential, with performance often assessed through the residence time distribution (RTD) parameter. RTD is used to trace material flow and behaviour within the mixing unit, providing insight into the mixing efficiency. The 3D-printed mixing setup was coupled with in-line near infrared spectroscopy (NIR), with the probe placed at the powder outlet enabling real-time monitoring of mixing efficiency. NIR is well-suited for in-line measurements as the method is quick, non-destructive and accessibility of inexpensive optical fibre probes, making it ideal for CM lines (De Beer et al., 2011). Accurate placement of the NIR probe within the system is crucial for ensuring blend uniformity and allowing for process parameter adjustments. Hirschberg et al. (Hirschberg et al., 2018b) further developed this approach by prototyping, via FDM-3DP, a specialised NIR spectroscopic calibration setup. This allowed for continuous powder mixing during calibration samples measurements (Fig. 1-B). This method facilitates optimization of manufactured geometries, including equipment size and the placement of process analytical interfaces, enhancing the efficiency and accuracy of CM processes.

2.2. Micro-fluidized bed

Micro-fluidized bed (MFB) is an innovative method that has been applied to engineering processing and screening because of its high mass/heat transfer, low cost, low reaction time, and efficient mixing. Solid screening, chemical conversion, CO_2 capture, wastewater treatment, and microbiological processing are just a few of the many applications for MFB (Zhang et al., 2021b). Various materials and fabrication techniques have been documented for the manufacture of MFB. The most popular method is the use of transparent quartz/glass capillaries, which enables clear visualisation analysis. However, there is growing interest in creating microfluidic devices using 3DP techniques. A microfluidized bed (15 × 15 mm in cross-section) was designed and fabricated with the use of the SLA-3DP by Zhang et al. (Zhang et al., 2021a) (Fig. 2-A). Similarly, McDonough et al. (McDonough et al., 2020) used the same manufacturing technique to miniaturize an already marketed swirling fluidized bed technology: TORBED (Fig. 2-B). The TORBED design utilises static angled blades to introduce a tangential velocity component, enhancing heat and mass transfer rates. The miniaturization of the TORBED device to a 50 mm diameter scale was made possible by 3DP. Traditional manufacturing methods would not have been able to produce the complex blade distributor geometry at this scale in a time-efficient or cost-effective manner.

2.3. Fluid mixing and spinning setups

Microfluidics (MF) and electrospinning are promising techniques

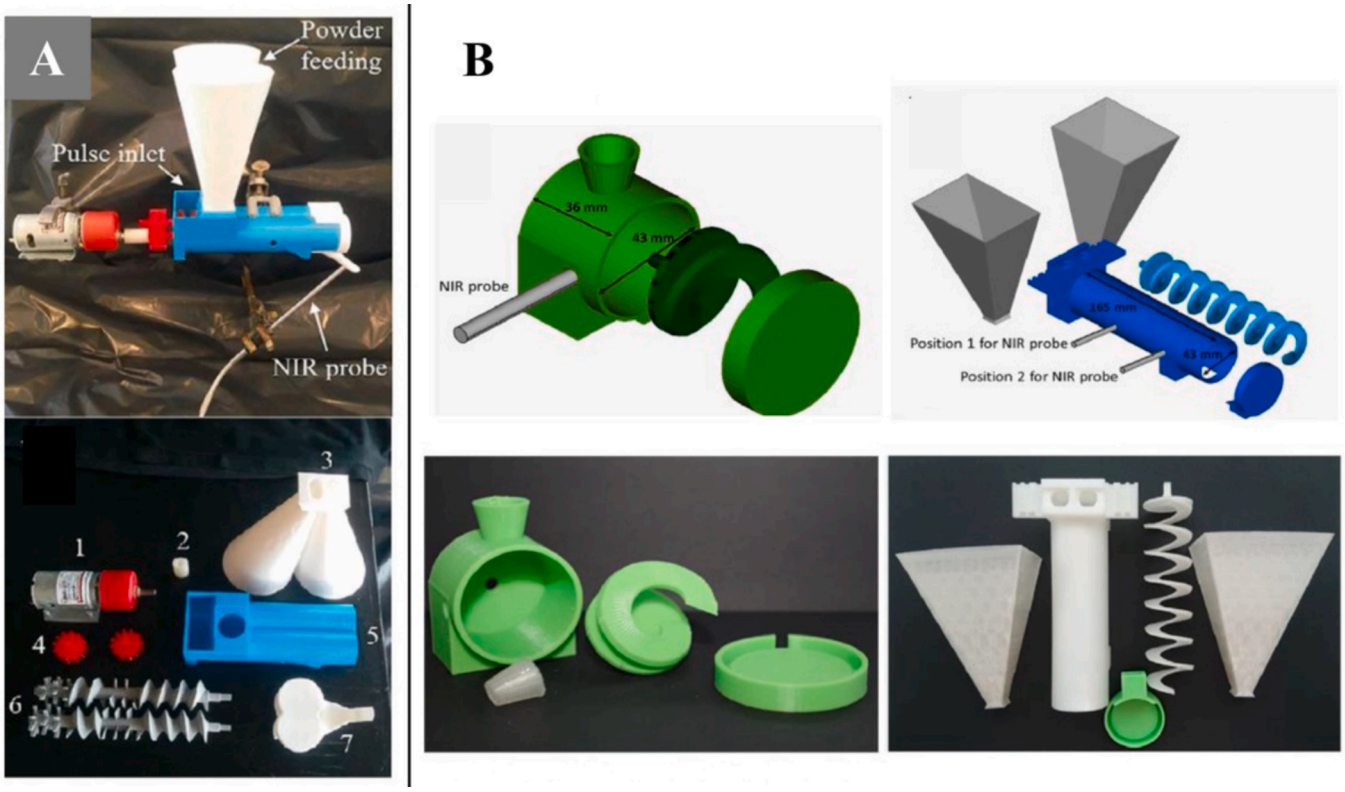

Fig. 1. Different 3D-printed mixing geometries for CM powder mixing setups. A) The assembled and disassembled experimental setup (1: Motor for rotating the twin screws, 2: Connection part between motor and sprocket, 3: Hopper with two feeding funnels, 4: Sprockets connecting active and passive screw, 5: Twin screw chamber, 6: Screw design, 7: Powder outlet). Reprinted with permission from (Svane et al., 2021). B) CAD of the calibration setup and the continuous single screw mixing prototype chamber and screw (upper panels), 3D-printed calibration setup, consisting of chamber, lid, screw and backstopper and 3D-printed single screw mixing prototype setup for continuous mixing (lower panels). Reprinted with permission from (Hirschberg et al., 2018b).

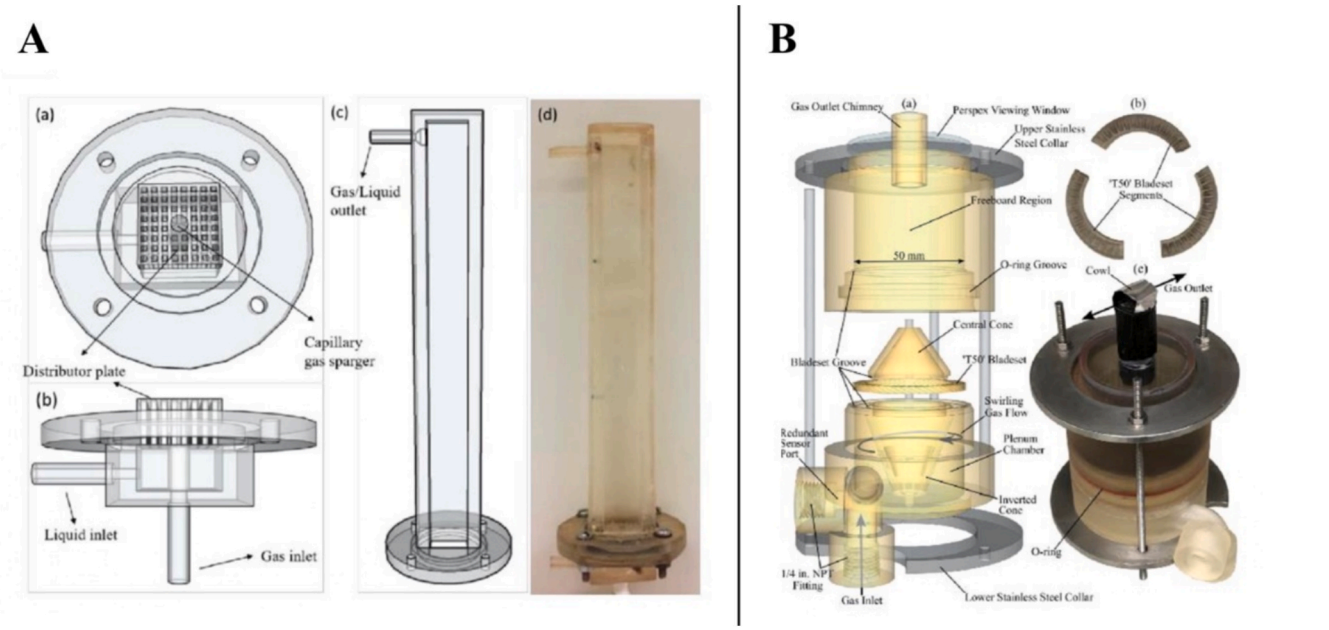

Fig. 2. Design of 3D-printed MFBs. A) CAD model of the MFB: (a) top view of the lower section, (b) front view of lower section, (c) upper main column with and (d) image of the assembled 3D-printed MFB. Reprinted with permission from (Zhang et al., 2021a). B) (a) CAD model of the small-scale TORBED, (b) 3D-printed T50 blade segments, (c) fully assembled 3D-printed high temperature polymer prototype. Reprinted with permission from (McDonough et al., 2020).

across various fields, predominantly in pharmaceuticals, where they have been widely applied in the development of drug delivery systems (DDS). Their advantages over traditional manufacturing methods include faster processing, ease of use, and enhanced control over the final product's characteristics. Additionally, these technologies offer excellent reproducibility and the potential for scaling up to continuous manufacturing. However, their adoption is often limited to well-equipped facilities due to the high cost of instruments. In this context, 3DP presents a valuable solution, to produce low-cost, simplified instrument setups, helping to overcome these challenges (Balakrishnan et al., 2021).

2.3.1. *Electrospinning setup*

Huang et al. (Huang et al., 2020) described the fabrication of a safe and low-cost electrospray/electrospinning setup by FDM. Consisting of a safety cap, a nozzle holder, a central chamber and an end part (Fig. 3), the modular apparatus was fully printed in 6 days using polymers as PLA and PVA thus, cutting the costs from $17,000 – $300,000 USD to approximately $100 USD. Each section was separately printed and then assembled. The end part was also provided with air channels to ensure counter-flow air stream to enhance the evaporation rate of the solvent from the produced material. This 3D-printed setup was successfully employed by Ambrus et al. (Ambrus et al., 2019) to produce loratadine-loaded electro spun nanofibers.

2.3.2. *Microfluidic chips*

In MF, the chip is the core component, typically consisting of multiple inlets for reagents, etched or moulded internal channels and an outlet for collecting the product. These channels connect the inlet to the outlet, facilitating passive or active micro mixing of fluids. Researchers have increasingly adopted 3DP for creating customized chip designs. By modifying the chip's internal structure, such as incorporating geometric impediments, the flow can be tailored to achieve different outcomes. The applications of 3D-printed chips in MF are diverse, from pharmaceutical manufacturing to biological testing. They are used to produce nanomedicines (*e.g.*, liposomes, polymeric nanoparticles), droplet emulsions, crystallisation and *in vitro* testing platforms like organs on chip. Different materials (*e.g.*, thermoplastic polymers, resins) and 3DP techniques (*e.g.*, FDM, SLA, Digital Light Processing DLP) have been explored, demonstrating the effectiveness of 3DP in chip manufacturing.

Tiboni et al. (Tiboni et al., 2021b) developed two different chip designs to achieve effective passive micro mixing: the "zigzag" and "split and recombine" designs (Fig. 4-A). Using FDM, they created highly affordable chips made of polypropylene (PP), a flexible, chemically inert

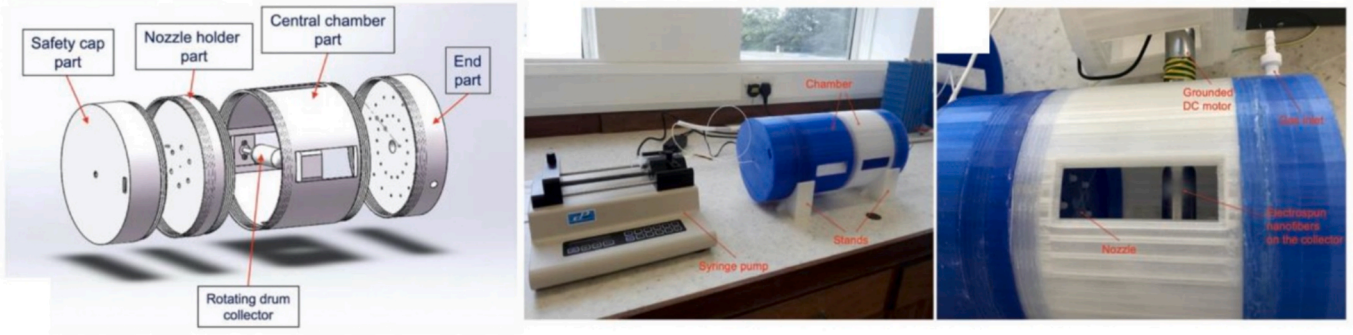

Fig. 3. CAD of the electrospray/electrospinning chamber with the rotating drum collector and the 3D-printed setup with two chamber parts assembled in electrospray mode. Reprinted with permission from (Huang et al., 2020).

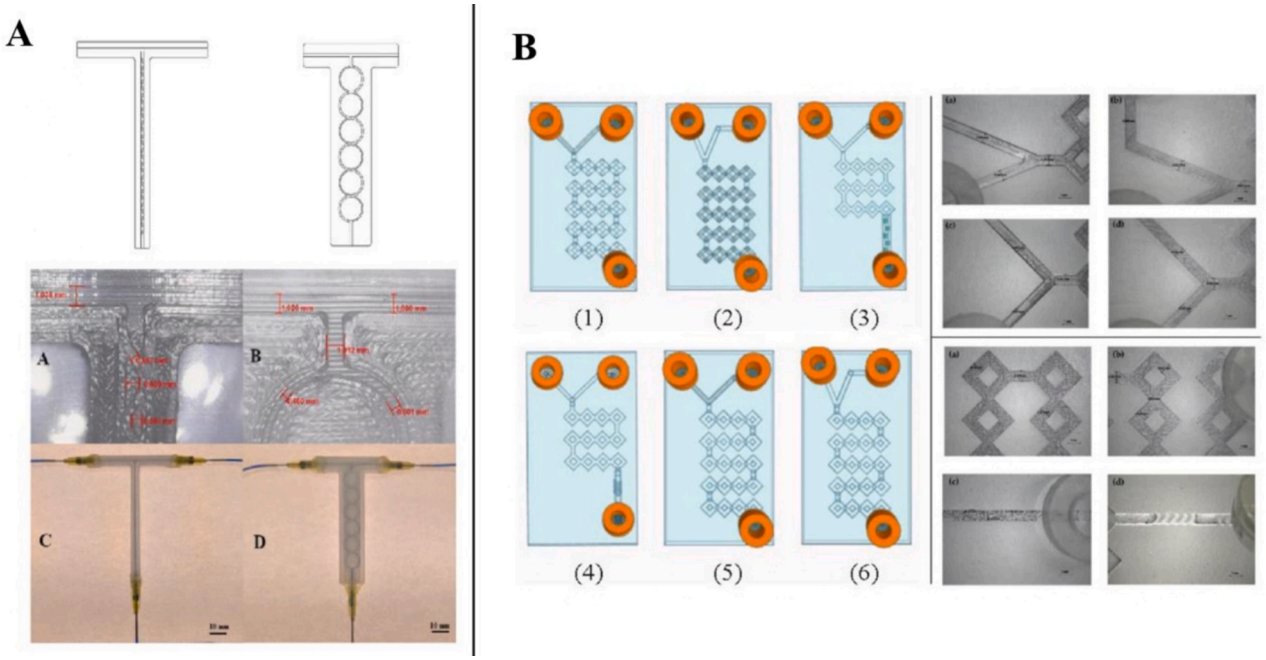

Fig. 4. 3D-printed MF chips and their internal designs. A) Computer aided design models of "Z" (zigzag design) and "C" (split and recombine design) microfluidic chips. Channel dimensions of the Z chip (A) and C chip (B). Coloured aqueous solution running through the two printed chips (C and D). Reprinted with permission from (Tiboni et al., 2021b). B) Schematic representation of the (1–6) devices' CAD design and optical microscope images of DLP 3D-printed devices (8 ×). Upper panel: (a) inlet's image of device 2, (b) inlet's image of device 6, (c) inlet's image of device 1, (d) inlet's image of device 5. Lower panel: (a,b) image of the mixing microchannels, (c) image of wedges (device 3), (d) image of the modified herringbone structure (device 4). Reprinted with permission from (Sommonte et al., 2022).

material resistant to most solvents used in microfluidics. These 3D-printed chips were characterized by computational fluid dynamics (CFD) studies and successfully applied to produce cannabidiol-loaded lipidic and polymeric nanocarriers with tuneable properties. Sommonte et al. (Sommonte et al., 2022) designed 3D-printed diamond-shaped chips using DLP with PlasCLEAR^{TM} resin (Fig. 4-B) and used these high-resolution, ready-to-use, reusable chips to manufacture PEGylated liposomes loading lysozyme as a model enzyme.

3D-printed MF chips are increasingly used to create cost-effective devices due to their remarkable ability to enhance fluid mixing and particle size control. The ability to deposit stable, patterned, and complex structures has the potential to serve as a foundation for large-scale manufacturing of materials with intricate designs, such as artificial cell models. Other examples on how 3D-printed MF chips can be employed were given by Li et al. (Li et al., 2020a) who developed single-step 3D-printed MF devices to produce multiphase emulsions with a user-defined chemical and morphological organization. Specifically, FDM was employed to manufacture a chip featuring multi-material channels made from both hydrophilic (PVA) and hydrophobic (PLA) materials. This configuration allowed to generate o/w and w/o droplet, which in turn formed complex water-in-oil-in-hydrogel triple emulsions in a single step. These droplets templates can incorporate lipid bilayers and membrane proteins, providing not only stabilization and compartmentalization of neighbouring droplets, but also interaction between different environments.

Kara et al. (Kara et al., 2023) employed SLA 3D-printed MF chips to control the habit and polymorphism of sulfadimine (SDM): 4-aminosalycilic acid (4ASA) cocrystals. Tuning the flow rate and using high surface-to-volume ratio microchannels enables a more homogeneous and rapid mixing process. Moreover, having the chip in-line with the fluidized bed allowed mixing, coating and drying to occur in one single step, to obtain a CM of SDM:4ASA cocrystal-coated particles.

3. 3D printing for designing and manufacturing inhaler devices

The use of 3DP has also revolutionized the scenario of dose-dispensing devices manufacturing such as the case of inhaler devices, offering unparalleled flexibility and customization. By enabling the rapid prototyping of complex geometries, 3DP allows for the development of more efficient and patient-specific inhalers, tailored to optimize drug delivery to the lungs. This technology streamlines the production process, reduces material waste, and facilitates the testing of new designs, enhancing performance and reducing time-to-market. Additionally, 3DP opens new possibilities for creating devices with integrated smart features such as acoustic-driven devices that guide the patient inhalation, potentially improving user adherence and treatment outcomes. Still, this research area remains largely underexplored, as evidenced by the limited number of studies published on this topic up to date.

3.1. Dry-powder inhalers (DPI)

A prime example of application of 3DP for inhaler devices is seen in dry-powder inhalers (DPIs), which are commonly used to deliver powder formulation to the lungs. Different types of DPIs exist, including unit-dose; multiple unit-dose or reservoir devices. The dispersion of powder in DPIs is triggered by a turbulent flow, which depends not only on the device design but also on the user's inspiratory effort. This inspirational force is crucial for proper drug administration. However, inhalation capacity can vary significantly among individuals, such as children, the elderly, or those with chronic respiratory conditions. In this context, adapting the design of DPIs becomes essential to ensure efficient aerosolization and delivery for patients with limited inspiratory capacity.

Ye et al. (Ye et al., 2023) investigated how the design of a capsule-based inhaler affects its performance. The device was entirely 3D printed, and various dimensions of its spiral channel, mouthpiece and air inlets were evaluated though CFD simulations (Fig. 5) and compared with the already marketed Breezehaler®. The designed DPIs were provided with an inner spiral channel for optimized airflow and enhance the detachment of active pharmaceutical ingredients (APIs) particles from their carrier. The study found that reducing the diameters of the

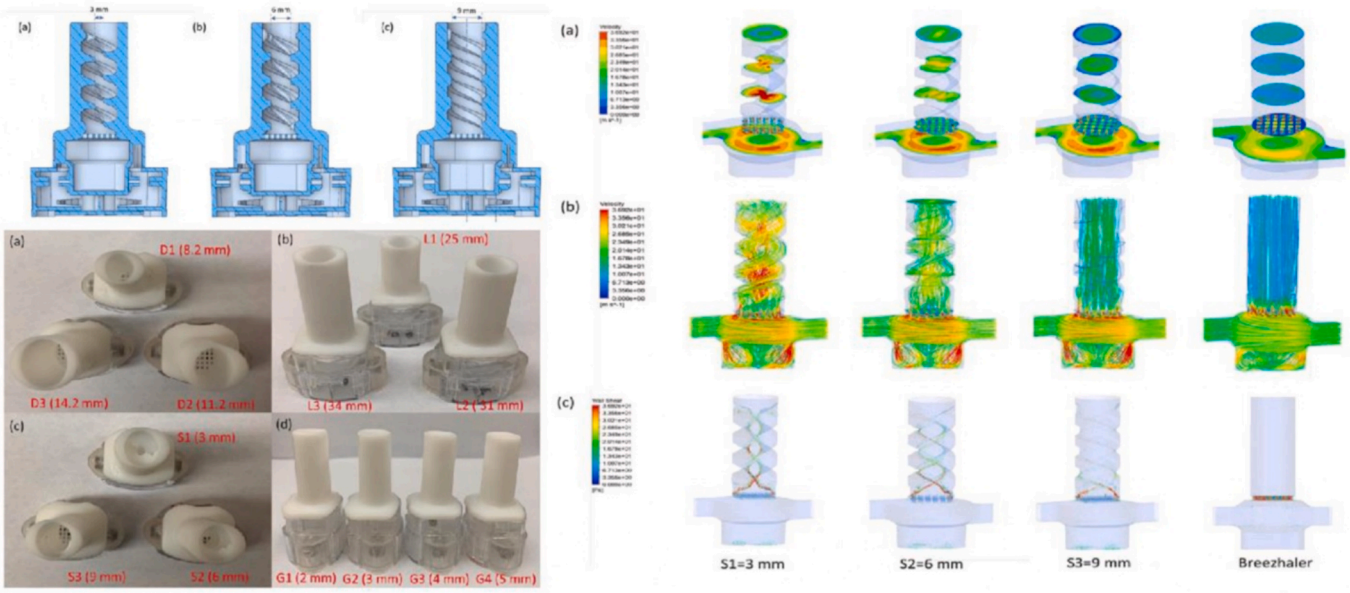

Fig. 5. 3D-printed DPIs. The 2D diagrams of inhalers with spiral channel designs in the mouthpiece: (a) 3-mm spiral channel, (b) 6-mm spiral channel, and (c) 9-mm spiral channel. 3D-printed inhalers with different design features: (a) inhalers with different mouthpiece diameters (D series), (b) inhalers with different mouthpiece lengths (L series), (c) inhalers with different diameters of spiral channel (S series), and (d) inhalers with different gas inlet widths (G series). The three inhalers designated as D2 (8.2 mm), L2 (31 mm), and G3 (4 mm), are the same inhaler without design modifications, identical to the commercial Breezhaler®. Contour maps of the inhalers with different inner diameters of spiral channels: (a) velocity profiles, (b) velocity streamlines, and (c) shear stress on the wall. Reprinted with permission from (Ye et al., 2023).

mouthpiece and air inlets increased turbulent airflow and gas velocity, resulting in more efficient drug-carrier detachment, powder deagglomeration, and improved aerosolization performance. However, the swirl design of the inner channel caused a higher drug retention within the device, probably due to the tangential flow associated with the swirl pipe.

Li et al. (Li et al., 2020b) designed an innovative capsule-based acoustic DPI (ADPI) using FDM-3DP. This smart inhaler helps guide the patient in the proper use of the device and monitor the drug administration process to ensure the correct dosage is delivered. The DPI is equipped with an acoustic component that generates a distinct sound signal when the user inhales at a specific flow rate, providing real-time feedback on inhalation performance.

Not all patients can generate the minimum required inspiratory flow rate or force necessary for effective dose delivery. Enhancing airflow through the device is crucial to ensure proper DPI dose delivery, regardless of the user's inspiratory capacity. Suwanpitak et al. (Suwanpitak et al., 2022) developed an "add-on" system using FDM 3DP to address this issue. The device was designed to be easily attached to the outside of the marketed Accuhaler® device and incorporated a centrifugal fan to enhance air flow into the device (Fig. 6). Computational fluid dynamics analysis showed that the add-on increased the amount of delivered dose of 15–20 %.

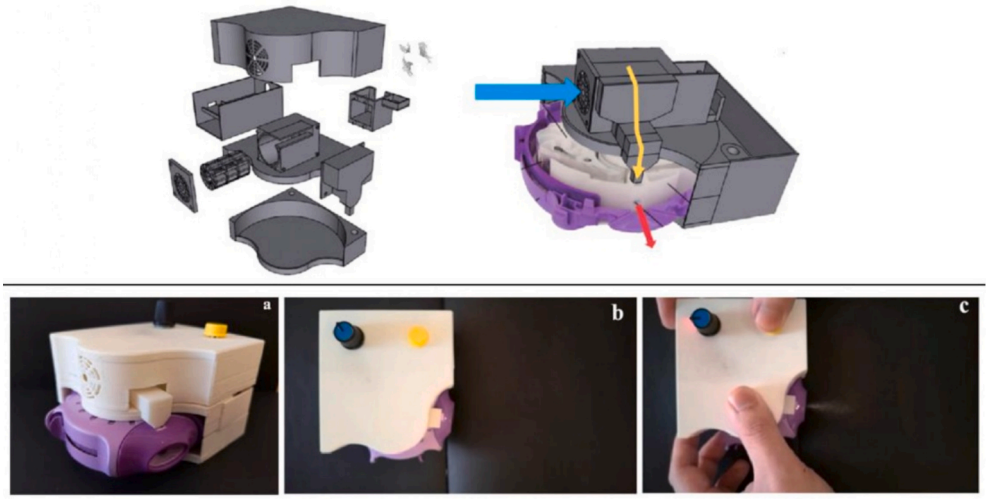

Fig. 6. 3D-printed DPI "add-on" device CAD model design and the assembled system: (a) assembly of the 3D printed add-on device and Accuhaler and (b,c) expulsion of drug from the Accuhaler® upon actuation of the yellow button on the add-on equipment. Reprinted with permission from (Suwanpitak et al., 2022). (For interpretation of the references to colour in this figure legend, the reader is referred to the web version of this article.)

3.2. Other customizable 3D-printed dose dispensing devices

Orodispersible films (ODFs) and graduated dosing dispensers are other additional examples of devices that allow for easy and customisable dosage adjustments for individualized therapy. Niese et al. (Niese et al., 2019) developed a flexible dispensing device for warfarin-loaded ODFs using FDM 3DP with PLA, ensuring the system meet Pharmacopoeia standards. The device offers high dosing accuracy, and 3DP enables both low production and development costs. The preformulated, sealed ODF is stored on a roll, which moves through the dispensing mechanisms. As the packaging foils are opened, they are rolled onto waste reels, while the ODF is released and exits through a slot. Since the amount of drug delivered is based on the length of the film dispensed, patients can easily manage their own dosing.

For powdered medication, accurate dosing can be a challenge. For this reason, Dobocan et al. (Dobocan et al., 2022) 3D printed a graduated dispenser designed for easy powder filling and precise dosing. Specifically, the device was developed for children with phenylketonuria, who require tailored doses of amino acid substitutes based on body weight.

4. 3D printing for customizable laboratory instrumentation

Advancements in manufacturing technologies, such as 3DP, have contributed to a significant rise in the "do-it-yourself" (DIY) approach. The increased availability of affordable 3D printers has made in-house production more common, not only in everyday life but also within laboratory settings. The DIY approach is particularly appealing to researchers as it allows for easy customization of devices to meet specific experimental requirements.

4.1. 3D-printed tools for dissolution apparatuses

Most dissolution methods rely on widely accepted procedures, such as the United States Pharmacopoeia (USP) dissolution apparatuses. However, no standard testing conditions have been established for the assessment of drug release of unconventional oral dosage forms. Given the large volume and surface area involved in gastrointestinal (GI) absorption, these USP methods use large dissolution chambers that create sink conditions mimicking the GI's tract's environment. However, for smaller regions like the buccal cavity, lungs, or periodontal areas, these large chambers fail to provide appropriate testing conditions.

To address this, Ren et al. (Ren et al., 2019) developed a small flow-through cell (0.04 mL inner volume), more physiologically relevant for assessing drug release in periodontal delivery. SLA-3DP was used in the device's manufacturing processes. Drug release tests were conducted using a commercially available long-acting periodontal insert, and computer simulations were employed to model diffusion and assess the impact of various factors on the dissolution profile before conducting experimental studies. Wanasathop et al. (Wanasathop et al., 2022) also used a modified version of this device to test other periodontal medications. Key additions included a temperature-controlled sampling chamber, a filtration system, and blocking film to accommodate the unique characteristics of the dosage forms. This method proved effective to assess drug release from periodontal dosage forms in a biologically relevant environment, offering sufficient dose discrimination for manufacturing and quality control (QC) purposes.

Dorozynski et al. (Dorożyński et al., 2018) 3D printed a specific tablet holder for drug release studies. The insert was designed on the inner characteristics of the flow-through cell of a USP dissolution apparatus to test the release profile of a mucoadhesive buccal formulation (Fig. 7). Moreover, the device was also intended to be Magnetic Resonance Imaging (MRI)-compatible to capture real-time images during hydration of the tablet in the dissolution medium. Similarly, Speer et al. (Speer et al., 2019) designed a PLA-3DP tool to hold Oro dispersible films during dissolution studies and adapted it to the flow-through cell dimensions. A total inner volume of 3.2 mL, comparable to that of *in vivo* human saliva, was used and ODFs with immediate and prolonged release as well as double-layer films were investigated.

4.2. 3D-printed Franz cells

The first fully 3D-printed transparent Franz cell was developed relatively recently, in 2018 by Sil et al. (Sil et al., 2018), using an SLA 3D printer. Franz cells are commonly used to assess *in vitro* drug release and permeation profile of topical formulations. Traditionally made from fragile borosilicate glass, the cells consist of two chambers, donor and receptor, separated by a polymeric or biological membrane. Due to the fragility and high costs of these cells, the possibility of "in house" fabrication using 3DP has drawn significant interest. Tiboni et al. (Tiboni et al., 2021a) also developed vertical static diffusion cells (VDCs), in compliance with Pharmacopoeia standards. They used FDM

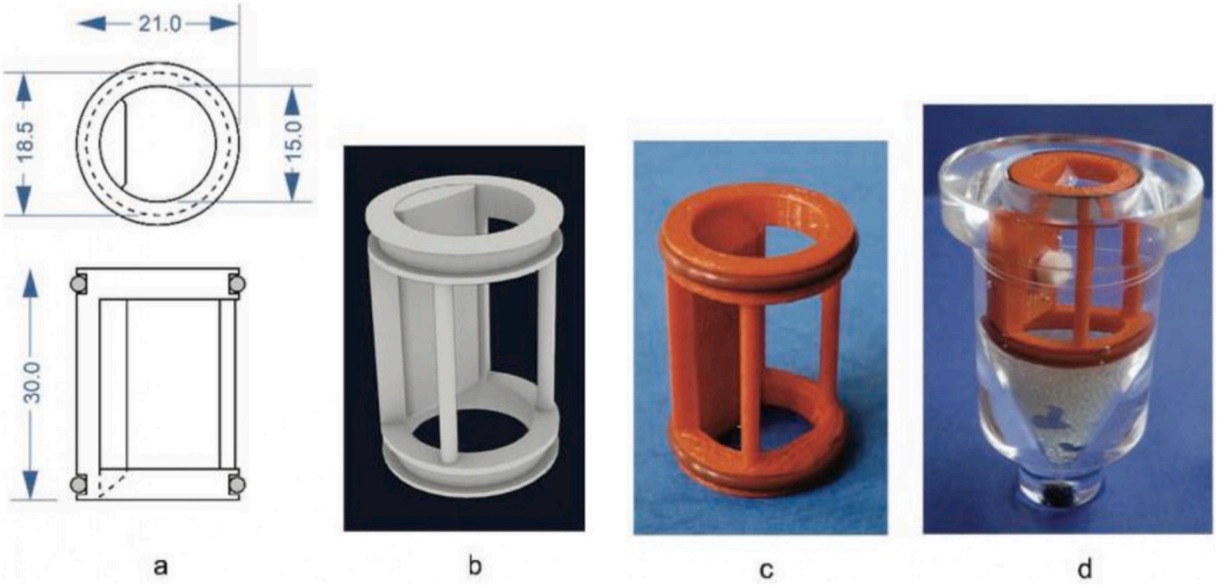

Fig. 7. Customized 3D-printed dissolution apparatus. (a,b) the design of the insert/holder for buccal tablets, (c) 3D-printed insert, (d) insert with the tablet fitted inside the flow-through cell. Reprinted with permission from (Dorożyński et al., 2018).

3DP with polypropylene (PP) as chosen material due to its durability, flexibility and chemical resistance to many organic solvents. Moreover, to eliminate the need for a warm water recirculatory system for temperature control, the dimensions of the cells were specifically designed to fit in a dry heating block (for 15 mL centrifuge tubes), as shown in Fig. 8-A.

Other devices resembling conventional Franz cells have also been produced through 3DP. Suarato et al. (Suarato et al., 2018) used FDM with PLA to create a "pocket size" diffusion cell (3D-PDC) for skin permeation tests (Fig. 8-B). The compact design of the device not only reduces the material consumption and waste but also offers easy integration with other analytical instruments, such as microscopy or spectrometry, for real-time drug detection in tissue samples.

Similarly, Ding et al. (Ding et al., 2019)developed a miniaturized multichannel device (MCDs) using SLA-3DP (Fig. 8-C). The small dimensions of these devices minimise the use of skin tissues and drug samples required, significantly reducing costs. Additionally, their multichannel design enables simultaneous replicate analyses, saving both time and resources. When validated against conventional diffusion cells, the 3DP devices proven to be a reliable alternative for *in vitro* skin permeation analysis.

Fazili et al. (Fazili et al., 2020) also developed a specialised 3D printed Franz cell-like device equipped with UV-imaging capabilities. To enable real-time UV imaging, they incorporated a quartz dose tube and quartz window into the PLA device. The 3D-printed apparatus provided successful results, demonstrating the potential to eliminate the need for additional analytical techniques like HPLC. However, careful selection of the manufacturing material is crucial to prevent issues such as leakage and interactions with the sample under analysis.

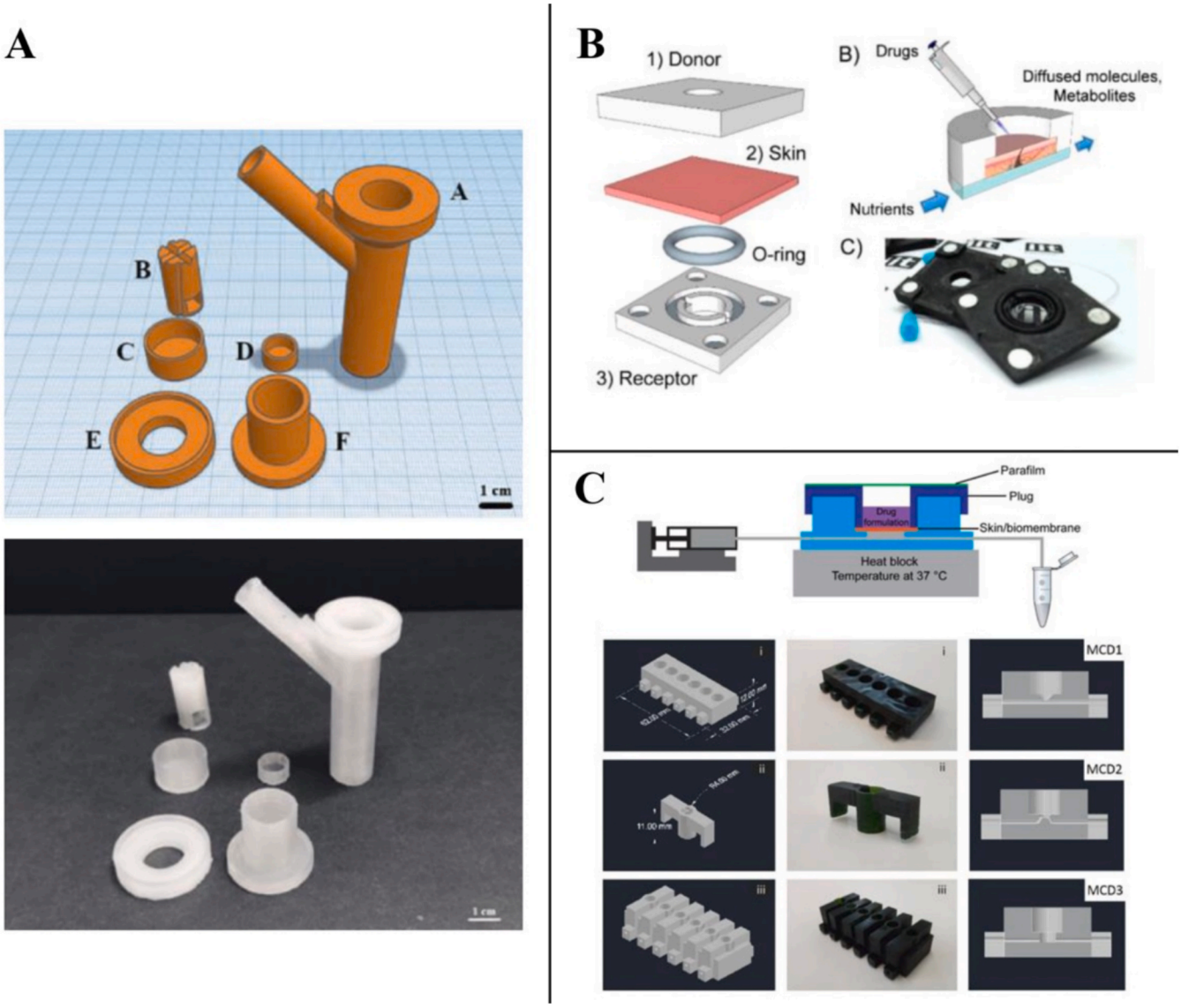

Fig. 8. 3D-printed diffusion cells. A) CAD design of the VDC parts and polypropylene 3D-printed parts: (A) receptor compartment with withdrawal window, (B) stirring block; (C) cap for donor compartment for liquid formulations, (D) cap for withdrawal window, (E) donor compartment for semisolid formulations, (F) donor compartment for liquid formulations. Reprinted with permission from (Tiboni et al., 2021a). B) Schematic representation of the 3D-PDC that consists of three parts: (1) the receptor chamber, integrating two channels and a glass window, (2) the skin tissue and (3) the donor chamber. An O-ring inserted under the skin seals the receptor and prevents leakage of liquids. Both components integrate 4 magnets to ease the assembling procedure; (B) 3D-PDC operational principle; (C) photograph of the donor and receptor parts (3D-PDC size 1 cm × 3.5 cm × 3.5 cm). Reprinted with permission from (Suarato et al., 2018). C) Schematic representation of the MCD diffusion system (Side view of the diffusion cell). The CAD schematic representations of the MCD design and the various designs of receptor chambers. i): the bottom with receptor chamber; ii): the top inset with donor compartment; iii): the overview of whole device. Reprinted with permission from (Ding et al., 2019).

4.3. Other customized 3D-printed analytical tools

In-situ gelling formulations represent an innovative approach to drug delivery, utilising physiologically responsive polymers. The rheological properties of these formulations, such as gelation or dissolution, play a significant role in drug release from the matrix. These changes occur upon contact of the formulation with physiological fluids at varying pH level and ion concentrations, making it essential to control the sol–gel transition to optimize the formulations for specific therapeutic goals. Senjoti et al. (Senjoti et al., 2020) developed a method for monitoring rheological changes when formulations interact with physiological fluids while simultaneously evaluating the drug release profile. This was achieved through the creation of a rheo-dissolution cell that can be attached to the lower plate of a rheometer. The device was manufactured using FDM-3DP with acrylonitrile butadiene styrene (ABS) and features a circular reservoir with a top opening covered by a stainless-steel mesh during the experiments. The cell includes inlet and outlet ports for loading and sampling from the 55 mL reservoir.

Fourier transform infrared spectroscopy (FTIR) is a rapid analytical technique that offers non-destructive, molecule-specific qualitative and quantitative data. Attenuated total reflection (ATR) setup is the most widely used probing approach for obtaining IR spectra as it enables rapid and reliable measurements of liquids, solids, pastes, and other more complex samples. A fully 3D-printed ATR module for ATR-FTIR spectroscopy was manufactured by Baumgartner et al. (Baumgartner et al., 2020). Cost-efficiency, robustness, and ease of sample application are the main features of the device that was designed to fit in commercially available FTIR instruments. The versatility of 3DP enabled customization of the instrument for specific analytical requirements, allowing its use in diverse settings, including hazardous biological samples and quantitative liquid investigations with a 3D-printed liquid compartment.

Determining the dose that reaches the lung for therapeutic efficacy involves the use of standard Pharmacopoeia impactors such as the multi-stage liquid impinger, next generation impactor (NGI), and Anderson cascade impactor (ACI). However, a lack of meaningful data regarding drug dissolution and transport at the lung epithelia has hindered the development and optimization of novel inhaled formulations in the pre-clinical stage. This is primarily due to the absence of physiologically relevant *in vitro* respiratory models. Wong et al. (Wong et al., 2022) modified a standard NGI through the integration of modified 3D-printed plates. These were specifically designed to accommodate three cell culture inserts representative of bronchial and alveolar epithelia and were put at stage 3 and 7 of the NGI apparatus. Resveratrol dry powder with a respirable particle size was chosen as the model formulation and its performance compared to a conventional instrument. This set up provided valuable insights into drug absorption and transport across lung epithelia highlighting the importance of enhancing *in vitro* respiratory models in a physiologically relevant manner. Pozzoli et al. (Pozzoli et al., 2016) developed a custom-made expansion chamber (MEC) using FDM-3DP with ABS material. RPMI 2650 nasal cell epithelia were incorporated on Snapwell cell inserts within the MEC, which was attached to a cascade impactor to assess drug deposition and permeation using a commercially available budesonide nasal spray, Rhinocort®. The inclusion of RPMI 2650 nasal cell improved the representation of the mucosal surface present in the nose. The cell inserts were then removed from the modified chamber and transferred into a 6-well plate containing Hank's Buffered Salt Solution for drug transport testing. The new 3D-printed apparatus that incorporates cells demonstrated its effectiveness as an *in vitro* model for testing the delivery of nasal medications.

5. 3D-printed anatomical models for drug delivery testing

The use of 3D-printed anatomical models for drug delivery testing represents a significant advancement in pharmaceutical research and development. These models provide highly accurate representations of human anatomy, enabling researchers to simulate and study drug release and absorption in a more physiologically relevant context. By utilizing patient-specific data, 3DP allows for the customization of models to reflect individual anatomical variations, which can enhance the predictive power of studied drug delivery systems and improving therapeutic outcomes.

The anatomical models are usually reconstructed from computed tomography (CT) of MRI scans through segmentation techniques using software like Adobe Photoshop, 3D slicer, Solidworks® or Creo® and the final model printed using various type of 3DP techniques.

5.1. Nasal models

Nasal deposition has been shown to be linked to pharmacokinetic outcomes. Developing an understanding of the complex nasal anatomy and inter subject variability can lead to a better understanding of where the drug will deposit after administration. Moreover, nasal cavity geometries and dimensions vary between individuals based on differences in their age, gender, and ethnicity. The variation may affect the nasal spray deposition. 3DP approach can fully represent the geometries and dimensions of individuals which helps for patient specific treatment design. SLA technique, which offers unparallel high resolution outcomes is the most common used for these purposes. Nasal casts, which are replicas of the human nasal cavity, have evolved from models made from cadavers to complex 3D-printed structures. They can be divided into areas of interest with the purpose of quantifying deposition. Wilkins Jr et al. (Wilkins et al., 2021) 3D printed anatomical replicas of infant nasal airways which were segmented into six defined regions: anterior, nasal cavity, olfactory, paranasal sinuses, adenoid, and throat through post-processing and segmentation of the nasal replicas. The SLA 3D-printed models were used to assess local intranasal vaccine delivery using Mucosal Atomization Nasal Device and understand the impact of breathing conditions and administration parameters. Moraga-Espinoza et al. (Moraga-Espinoza et al., 2018) developed 3D-printed three human nasal airway replica casts based on CT-scans from a 7-year-old female, 12-year-old female, and 48-year-old male. Each cast was divided into five different areas (Fig. 9-A) that can be disassembled to facilitate drug recovery: the anterior region, which includes the vestibule and nasal valve area; the turbinate region, which is further divided into lower, middle, and higher sections. The casts were developed through SLA-3DP and used to study the regional deposition from the nasal sprays under different conditions. Similarly, Warnken et al. (Warnken et al., 2018) used 3D-printed nasal cavity replicas, developed based on the CT-scans of five paediatric and five adult subjects, to evaluate the deposition pattern from formulations producing a variety of plume angles. Casts were 3D printed using SLA and segtmented into five different sections: A-anterior, U-upper turninat regaion, M−middle turbinate regain, L-lower tubinate region, and N-nasopharynx, to qun-titiate the deposition patter within the nasal cavity. Sawant et al. (Sawant and Donovan, 2018) performed *in vitro* assessment of spray deposition patterns by using 3D-printed nasal cast based on MRI images obtained from a 12-year-old child's nasal cavity. The cast was segmented into five isolated vertical sections, each with a thickness of 1.7 cm. Calmet et al. (Calmet et al., 2022) developed and validated a SLA 3D-printed nasal model which was sectioned into anterior, middle and posterior sections (Fig. 9-B). A sensitivity test on nasal spray deposition across the different sections of the nasal cavity was conducted. The analysis demonstrated that the deposition in the anterior and middle sections is influenced by both the injection angle and breakup length, while deposition on posterior section is primarily, and significantly, affected by injection velocity. Compared to systemic drug administration, the nasal route provides a unique opportunity for brain targeted drug delivery via the olfactory and trigeminal pathways, resulting in effective drug delivery to the central nervous system (CNS). Nodilo et al. (Nodilo et al., 2021) applied a 3D-printed multi-sectional nasal cavity

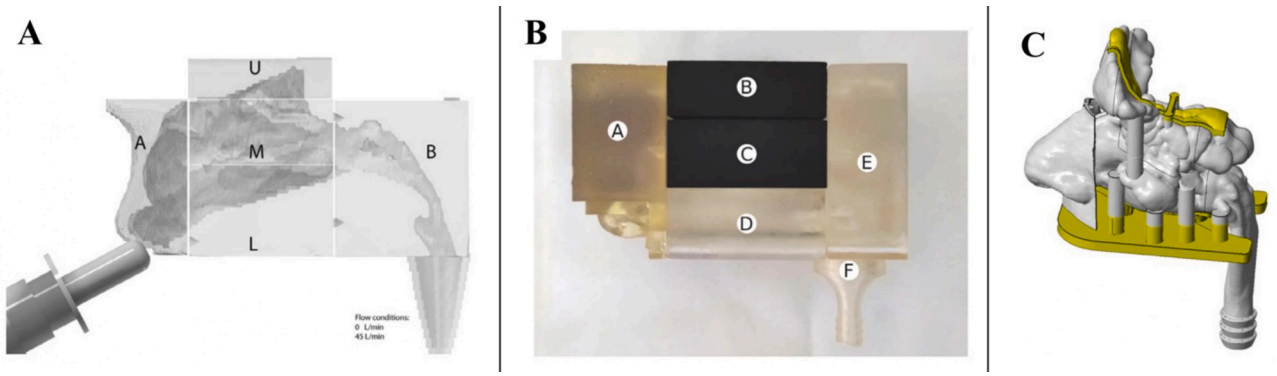

Fig. 9. 3D-printed nasal models and casts for drug delivery studies. A) Representation of the human nasal airway replica casts sectioned for regional deposition analysis. (A = anterior, U = upper turbinate region, M = middle turbinate region, L = lower turbinate region, N = nasopharynx). Deposition patterns obtained under ow conditions (45 L/min) were tested with both nostril open and with only one nostril open. Reprinted with permission from (Moraga-Espinoza et al., 2018). B) 3D-printed nasal model. (A) the nostrils, (B) the olfactory zone, (C) the middle turbinates, (D) the lower turbinates and (E) the nasopharyngeal zone, and (F) the pump adaptor containing a filter. Parts (B) and (C) contains the soft nasal valve. The nostrils are also 3D-printed in flexible resin. Reprinted with permission from (Calmet et al., 2022). C) Schematic presentation of a 3D-printed nasal cavity model based on healthy patient's airways reconstruction. Reprinted with permission from (Nodilo et al., 2021).

model to test their sprayable brain targeting powder. The multi-sectional SLA 3D printed nasal cavity model (Fig. 9-C) enabled precise determination of drug deposition in the regions of interest demonstrating that nasal cavity asymmetry affects drug deposition.

Dong et al. (Dong et al., 2020) assessed three types of intranasal nebulization devices by measuring the deposition of staining dye (methylene blue solution) in FDM 3D-printed models of the paediatric and adult nasal cavity (Fig. 10) with septal deviation and postsurgical paranasal sinuses. Acoustically driven nebulized drug delivery is the most efficient non-invasive technique for drug delivery to maxillary sinuses. Pourmehran et al. (Pourmehran et al., 2020) investigated the impact of geometrical parameters on the resonance frequency of the nose–sinus using a 3D-printed nasal casts to determine the resonance frequency of an idealized nose–sinus model. Owning to the transparency of the employed printing material, the 3D-printed model had the advantage to allow studying the drug distribution in the model visually. Xi et al. (Xi et al., 2016) adapted a Sar-Gel based colorimetry method to a 3D-printed sectional nasal airway cast, modelled from MRI data, to visualize deposition patterns and measure regional dosages. The study tested four nasal spray pumps and four nebulizers with both standard

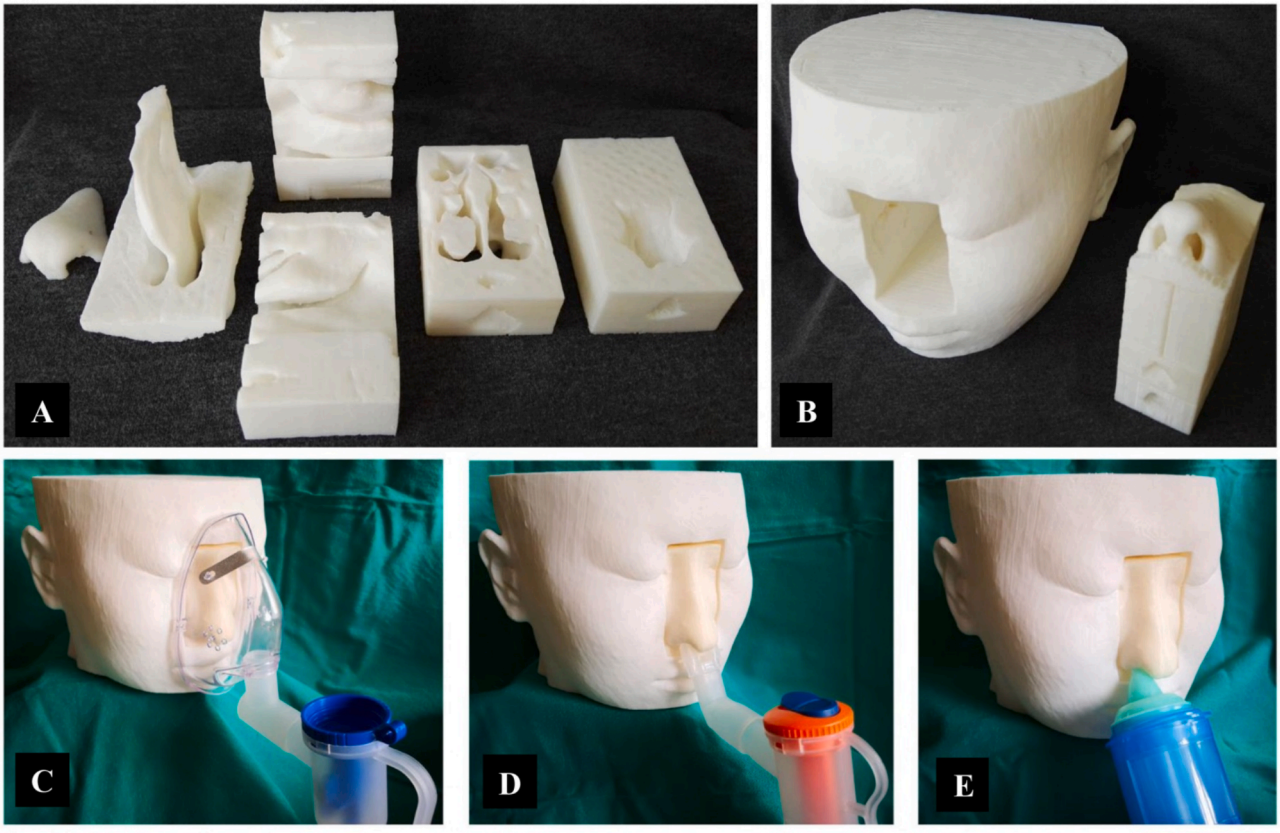

Fig. 10. 3D-printed nasal model for drug delivery studies: (A) Components of the nasal cavity, (B) Composed part of the nasal cavity and head mount, (C) Mask, (D) Double-headed nozzle. (E) Single-head nozzle. Reprinted with permission from (Dong et al., 2020).

and point-release administration techniques. Results indicated that standard nasal devices are insufficient to deliver clinically relevant doses to the olfactory region without significant drug losses in other nasal epitheliums.

Furthermore, the 3D-printed nasal models offer high flexibility in studying the impact of various parameters such as breath pattern, delivery device, formulation form etc. Van Strien et al. (Van Strien et al., 2021) developed, via SLA-3DP, a human nasal cavity model that was reconstructed from CT scans of a 48-year-old Asian male through segmentation techniques. The pressure distribution and the overall pressure drop in the nasal cavity were monitored through three ports along the nasal cavity floor, four on the lateral walls of both sides of the nasal cavity (fourteen in total), and two additional posterior ports at the nasopharynx. This model was applied to study the impact of the unsteady nature of inhalation (at flow rates of 10 L/min, 15 L/min, 20 L/min, and 30 L/min) on drug deposition. A better understanding of airflow characteristics in the upper airway (UA) of the nasal cavity is crucial in investigating obstructive sleep apnoea, particle sedimentation, drug delivery, and many biomedical problems. Wu et al. (Wu et al., 2019) manufactured by 3DP a unique half-side transparent physical model of a normal UA based on realistic anatomical structures, which enable the direct visualization of air flow patterns in *in vitro* models by using the smoke-wire method.

5.2. Throat models

3DP has also been extensively used for developing more physical representative throat model. For inhalation drug characterization, the USP induction port simulating the mouth throat region is the recommended attachment for impaction studies to determine drug deposition patterns. However, as the USP port is a metallic tube with a 90° bend, the design of the port does not include the special geometrical features that are fundamental to accurately predicting the *in vivo* drug deposition in the throat region. Thanks to 3D printing techniques, models that more accurately represent the real throat geometries have been developed. Moreover, in some cases, the transparency of the material allows the direct visualisation of the drug deposition. Huang et al. (Huang et al., 2022) used a 3D-printed mouth-throat model (the USP throat and a realistic mouth-throat with Handihaler®) to evaluate the relative inhalation parameters that affect the deposition of inhaled aerosols, including mouth-throat morphology, airflow rate, and initial condition of emitted particles. Kaviratna et al. (Kaviratna et al., 2019) investigated various bio-relevant mouth-throat models including Alberta Idealized Throat (AIT), and different size VCU models using two metered dose inhaler (MDI) drug product. The study found out that the suspension MDI were more sensitive to geometric differences of the mouth-throat models than the solution MDI. These results suggest that *in vitro* characterization of MDI products can be influenced by many variables, including the type of formulation, the mouth-throat geometry, shape, internal space volume, and the material used to make the mouth-throat models.

Still, USP, AIT and VCU models do not allow the incorporating of *in vitro* cellular model to study the deposition of aerosol drugs targeted at the cellular level. 3DP enables the breakthrough in this area. Sheikh et al. (Sheikh et al., 2023) developed a novel VCU-modified throat model via SLA-3DP which allows incorporating Detroit 562 cells grown in the air liquid configuration to elucidate drug transport across the pharyngeal cells. Their work demonstrated the potential of the novel 3D-printed device integrated with optimised cellular models as a promising *in vitro* device to investigate the transport of orally inhaled drug therapies and predict their therapeutic efficacy in targeting the throat region.

5.3. Lung models

The use of 3D-printed lung models is crucial for advancing respiratory research and drug delivery development. These models provide anatomically accurate representations of human lung structures, allowing researchers to simulate airflow, particle deposition, and drug distribution in a controlled environment. Unlike traditional *in vitro* models, 3D-printed lungs can replicate patient-specific conditions, enabling more precise evaluations of inhalation therapies and disease treatments. This approach not only improves the prediction of clinical outcomes but also reduces the need for human trials and animal testing, leading to more ethical and efficient research.

Collier et al. (Collier et al., 2018) created and 3D printed two human airway models, one including and one excluding the oral cavity and upper airways, from MR and CT imaging using SLS technique (Fig. 11-A). These were used to validate CFD simulations of airflow in realistic airway models. The results showed strong agreement between 3D velocity maps from flow MRI and CFD simulations. In the model including the upper airways, both methods revealed a turbulent laryngeal jet flow that significantly impacted velocity profiles in the trachea. Ho et al. (Ho et al., 2019) developed and tested novel multi-material 3D-printed airway models for bronchoscopy simulation. Utilising material jetting 3DP and polymer amalgamation, they created anatomically accurate, life-sized, and flexible models (Fig. 11-B) based on anonymized human thoracic CT images from three patients: one healthy, a second with a tumour obstructing the right main bronchus and third with a goitre causing external tracheal compression. Lim et al. (Lim et al., 2021) fabricated, via FDM, a 3D-printed human upper respiratory tract model to assess the deposition pattern of salbutamol sulphate. This *in vitro* model, showing realistic *in vitro-in vivo* correlation, may provide opportunities for personalized medicine in special populations or disease conditions. Peterman et al. (Peterman et al., n.d.) leveraged SLA-3DP to generate patient-specific lung models for quantifying lobular pulmonary deposition *in vitro*. This system was made with a combination of commercially available and 3D-printed components and allows the flow rate through each lobe of the lung to be independently controlled. This experimental setup's versatility allows for customization to simulate a wide range of inhalation conditions, thereby enhancing the rigor and accuracy of preclinical therapeutic testing.

Independent lung ventilation (ILV) is a life-saving procedure in unilateral pulmonary pathologies. ILV is underused in clinical practice, mostly due to the technically demanding placement of a double lumen endotracheal tube (ETT). Moreover, considering the high risk, the determination of ventilation parameters for each lung *in vivo* is limited. Kramek-Romanowska et al. (Kramek-Romanowska et al., 2021) utilized FDM-3DP to produce highly accurate physical models of anatomical structures (Fig. 11-C) used for *in vitro* research to assess the influence of double-lumen ETT on the gas transport and mixing. Lee et al. (Lee et al., 2019) used realistic 3D-printed phantoms, fabricated from four CT images, to study a stereotactic body radiation therapy case for lung cancer. They compared the dosimetry impact and treatment delivery efficacy of phase-gated versus amplitude-gated volumetric modulates arc therapy. Sonnenberg et al. (Sonnenberg et al., 2021) developed a SLA 3D-printed symmetric bifurcating tree model using ABS. The model mimicked part of the human airway to quantify the regional deposition patterns of different delivery inhalable systems and was constructed to allow for repeated measurements of regional deposition using reusable parts.

5.4. Other 3D-printed anatomical models for drug delivery testing

Yea et al. (Yea et al., 2017) assessed the feasibility of using a 3D-printed patient-specific anthropomorphic head phantom for quality assurance (QA) in intensity-modulated radiotherapy (IMRT) (Fig. 12-A). Left and right contoured head phantoms were converted from *dicom* to *stl* format, and 3DP was performed using FDM. The study concluded that the 3D-printed phantom is highly feasible for patient-specific QA, particularly for complex radiotherapy procedures like IMRT. Exposure to particulate contaminants can cause serious adverse health effects. Deposition on the facial mucosa is an important path of exposure, but it

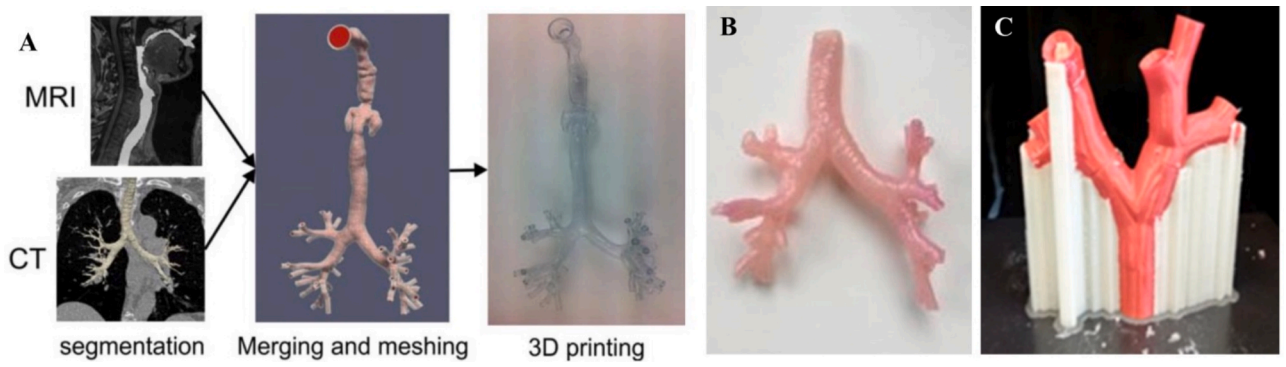

Fig. 11. 3D-printed lung models for drug delivery study. A) Workflow for the creation of the model including the upper airways and oral cavity derived from the segmentation of MRI images. Reprinted with permission from (Collier et al., 2018). B) 3D-printed normal tracheobronchial anatomy to the extent of the third order of bronchi (segmental bronchi). Reprinted with permission from (Ho et al., 2019). C) 3D-printed anatomical device to assess the influence of double-lumen ETT on gas transport and mixing. Reprinted with permission from (Kramek-Romanowska et al., 2021).

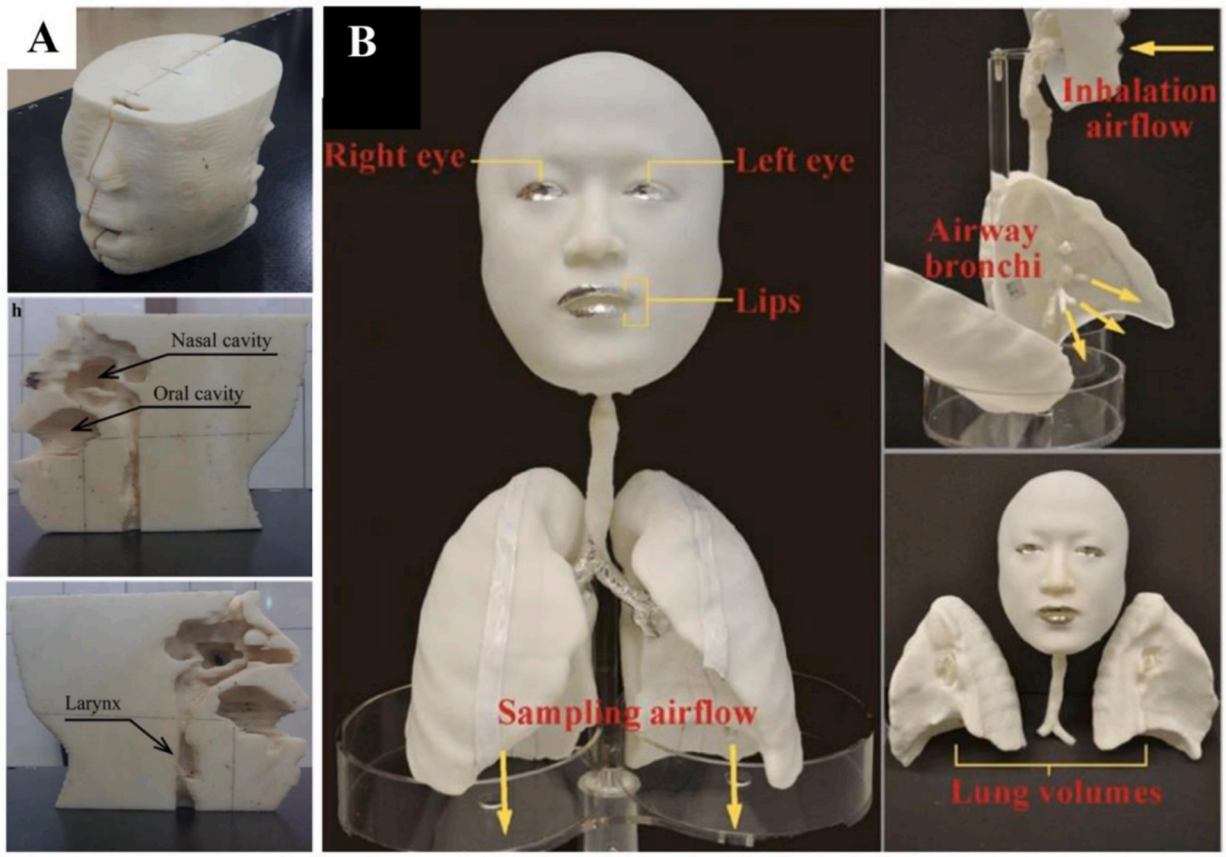

Fig. 12. Different anatomical 3D-printed models for drug delivery applications. A) Image of the 3D-printed anthropomorphic patient-specific head phantom including air cavities such as the nasal cavity, oral cavity, and larynx. Reprinted with permission from (Yea et al., 2017). B) 3D-printed *in vitro* face and airway model to assess the administered doses of micron-sized particles on the face mucosa. Reprinted with permission from (Duan et al., 2020).

is difficult to conduct direct dose measurement on real human subjects. For this purpose, Duan et al. (Duan et al., 2020) used a SLA 3D-printed realistic human model of facial mucosa, that includes a face, oropharynx, trachea, the first five generations of bronchi, and lung volume (Fig. 12-B), to assess the administered doses of micron-sized particles on the eyes and lips. The exposure dose of particles deposited upon the eyes and lips, quantified by fluorescence intensity, was determined via a standard wiping protocol.

Airway stents are used to manage central airway obstructions by restoring airway patency. Current stents are manufactured with standardized dimensions, and there are no stents that contain fenestrations required to maintain airway flow to bifurcations such as the right upper lobe (RUL) bronchus. Thus, these standard stents rarely contour perfectly to a patient's anatomy resulting in difficulty in choosing the best stent for a given patient. Xu et al. (Xu et al., 2021) adopted 3DP technique to develop a personalized airway model. Inspiratory computed tomography scans were obtained from 3 patients and analysed using 3D-Slicer™, Blender™ and AutoDesk® Meshmixer™ programmes to obtain working 3D-airway models. These 3D-printed modified models allowed for more precise stent customization, optimizing stent fit and allowing for cross-ventilation of branching airways.

6. Outlooks

3DP is often mentioned and has demonstrated its unparallel flexibility and customization. However, its environmental impact in pharmaceutical applications is also crucial. Studies have shown that 3DP can significantly reduce waste by its quick passage from concept to protype and use of precise amounts of materials, thereby minimizing costs, excess and scrap (Colorado et al., 2020). Additionally, 3DP processes often consume less energy compared to traditional manufacturing methods, contributing to a lower carbon footprint (Enemuoh et al., 2021; Yang et al., 2017) and the possibility to produce complex structures and geometries, along with formulations, locally further reduces transportation emissions, enhancing overall sustainability (Weaver et al., 2022). These factors collectively underscore the potential of 3DP to foster a more environmentally friendly approach in pharmaceutical manufacturing.

Moreover, given the clinical and industrial significance of 3DP, it is essential to address regulatory considerations that impact its application. Regulatory bodies such as the U.S. Food and Drug Administration (FDA) have begun recognizing and approving 3DP products (Thomas and West, 2018), ensuring they meet safety and efficacy standards. Compliance with Good Manufacturing Practices (GMPs) is crucial to maintain product quality and consistency. However, challenges in quality control persist, including the need for standardized protocols and rigorous testing to ensure the reliability and reproducibility of 3DP devices (Parhi, 2021). Moreover, a unique regulatory challenge arises when 3DP is performed at the point of care (PoC), such as in hospitals or clinics. The FDA is actively exploring frameworks to clarify these obligations and ensure that what is produced via 3DP is safe and effective (FDA, 2022). Features such as in-line quality control, camera monitoring, and automated verification systems are increasingly integrated into modern 3D printers to support GMPs requirements (Kayalar et al., 2023). Continued collaboration among regulators, manufacturers, and healthcare providers is essential to develop standardized protocols and ensure that 3D-printed products consistently meet the highest standards of quality, safety, and efficacy.

7. Conclusions

In summary, the rapid evolution of 3DP technologies has revolutionized the production of dosage forms and drug delivery systems in the pharmaceutical industry, with a strong emphasis on patient-centric care. One of the key advantages of 3DP is its ability to efficiently and intelligently create customized models and devices tailored to individual patient needs. This personalized approach enhances the precision and effectiveness of drug therapies, enabling the development of safer, more effective, and more suitable treatments for patients. At the same time, its potential to minimize material waste and streamline supply chains aligns with sustainability goals, fostering more environmentally responsible practices. This approach not only enhances healthcare outcomes but also promotes a more sustainable and innovative future for pharmaceutical manufacturing, paving the way for cost-effective, patient-centered, and eco-friendly solutions in the medical field. As the capabilities of 3DP continue to expand, its application in pharmaceutical manufacturing is expected to grow, offering new avenues for on-demand drug production and the ability to address inter-individual variability in drug responses. Despite its promise, significant challenges remain, particularly in the regulatory framework. Issues such as process standardization, quality control, and ensuring consistent product performance must be addressed to fully integrate 3DP into mainstream pharmaceutical practices. Overcoming these regulatory hurdles will be essential for realizing the full potential of 3DP in delivering advanced, patient-specific therapies.

CRediT authorship contribution statement

Costanza Fratini: Writing – original draft, Methodology. **Ye Zhang:** Writing – original draft, Methodology. **Sofia Moroni:** Data curation. **Mattia Tiboni:** Project administration, Data curation. **Hui Xin Ong:** Project administration, Data curation. **Paul M. Young:** Writing – review & editing, Resources. **Luca Casettari:** Writing – review & editing, Resources, Funding acquisition, Conceptualization. **Daniela Traini:** Writing – review & editing, Resources, Funding acquisition, Conceptualization.

Declaration of competing interest

The authors declare that they have no known competing financial interests or personal relationships that could have appeared to influence the work reported in this paper.

Acknowledgement

This work has been funded by the European Union - NextGenerationEU, Mission 4, Component 2, under the Italian Ministry of University and Research (MUR) National Innovation Ecosystem grant ECS00000041 - VITALITY – CUP H33C22000430006

Data availability

The authors are unable or have chosen not to specify which data has been used.

References

Ambrus, R., Alshweiat, A., Csóka, I., Ovari, G., Esmail, A., Radacsi, N., 2019. 3D-printed electrospinning setup for the preparation of loratadine nanofibers with enhanced physicochemical properties. Int. J. Pharm 567. https://doi.org/10.1016/j.ijpharm.2019.118455.

Balakrishnan, H.K., Badar, F., Doeven, E.H., Novak, J.I., Merenda, A., Dumée, L.F., Loy, J., Guijt, R.M., 2021. 3D Printing: an alternative microfabrication approach with unprecedented opportunities in design. Anal. Chem. https://doi.org/10.1021/acs.analchem.0c04672.

Baumgartner, B., Freitag, S., Lendl, B., 2020. 3D Printing for Low-Cost and Versatile Attenuated Total Reflection Infrared Spectroscopy. Anal. Chem 92, 4736–4741. https://doi.org/10.1021/acs.analchem.9b04043.

Calmet, H., Oks, D., Santiago, A., Houzeaux, G., Corfec, A.L., Deruyver, L., Rigaut, C., Lambert, P., Haut, B., Goole, J., 2022. Validation and Sensitivity analysis for a nasal spray deposition computational model. Int. J. Pharm 626, 122118. https://doi.org/10.1016/j.ijpharm.2022.122118.

Kayalar, C., Charoo, N.A., Nutan, M.T., Kuttolamadom, M., Khan, M.A., Rahman, Z., 2023. Quality Control and Regulatory Landscape of 3D-Printed Drug Products. AAPS Advances in the Pharmaceutical Sciences Series.

Chen, G., Xu, Y., Kwok, P.C.L., Kang, L., 2020. Pharmaceutical Applications of 3D Printing. Addit. Manuf. https://doi.org/10.1016/j.addma.2020.101209.

Collier, G.J., Kim, M., Chung, Y., Wild, J.M., 2018. 3D phase contrast MRI in models of human airways: Validation of computational fluid dynamics simulations of steady inspiratory flow. J. Magnet. Resonance Imaging 48, 1400–1409. https://doi.org/10.1002/jmri.26039.

Colorado, H.A., Velásquez, E.I.G., Monteiro, S.N., 2020. Sustainability of additive manufacturing: the circular economy of materials and environmental perspectives. J. Mater. Res. Technol. 9, 8221–8234. https://doi.org/10.1016/j.jmrt.2020.04.062.

De Beer, T., Burggraeve, A., Fonteyne, M., Saerens, L., Remon, J.P., Vervaet, C., 2011. Near infrared and Raman spectroscopy for the in-process monitoring of pharmaceutical production processes. Int. J. Pharm. https://doi.org/10.1016/j.ijpharm.2010.12.012.

Ding, D., Pan, J., Yeo, S.H., Wagholikar, V., Lim, S.H., Wu, C., Fuh, J.Y.H., Kang, L., 2019. A miniaturized device for biomembrane permeation analysis. Mater. Sci. Eng. C 103. https://doi.org/10.1016/j.msec.2019.109772.

Dobocan, C.A., Pop, E., Bogdan, M., Grec, C., 2022. Design and modelling a graduated dispenser for metabolic diseases—phenylketonuria. Appl. Sci. (Switzerland) 12. https://doi.org/10.3390/app122010672.

Dong, D., Cai, F., Huang, S., Zhu, X., Geng, J., Liu, J., Lv, L., Zhang, Y., Zhao, Y., 2020. Assessment of three types of intranasal nebulization devices in three-dimensional printed models and volunteers: a pilot study. Int. Forum. Allergy. Rhinol 10, 1300–1308. https://doi.org/10.1002/alr.22657.

Dorożyński, P., Jamróz, W., Węglarz, W.P., Kulinowski, W., Zaborowski, M., Kulinowski, P., 2018. 3D printing for fast prototyping of pharmaceutical dissolution testing equipment for nonstandard applications. Dissolut. Technol 25, 48–53. https://doi.org/10.14227/DT250418P48.

Duan, M., Liu, L., Da, G., Géhin, E., Nielsen, P.V., Weinreich, U.M., Lin, B., Wang, Y., Zhang, T., Sun, W., 2020. Measuring the administered dose of particles on the facial mucosa of a realistic human model. Indoor. Air 30, 108–116. https://doi.org/10.1111/ina.12612.

Enemuoh, E.U., Menta, V.G., Abutunis, A., O'brien, S., Kaya, L.I., Rapinac, J., 2021. Energy and eco-impact evaluation of fused deposition modeling and injection molding of polylactic acid. Sustainability. (Switzerland) 13, 1–15. https://doi.org/10.3390/su13041875.

Fazili, Z., Ward, A., Walton, K., Blunt, L., Asare-Addo, K., 2020. Design and development of a novel fused filament fabrication (FFF) 3D printed diffusion cell with UV imaging capabilities to characterise permeation in pharmaceutical formulations. Eur. J. Pharm. Biopharm. 152, 202–209. https://doi.org/10.1016/j.ejpb.2020.05.013.

Hirschberg, C., Boetker, J.P., Rantanen, J., Pein-Hackelbusch, M., 2018a. Using 3D Printing for Rapid Prototyping of Characterization Tools for Investigating Powder Blend Behavior. AAPS. PharmSciTech 19, 941–950. https://doi.org/10.1208/s12249-017-0904-0.

Hirschberg, C., Schmidt Larsen, M., Bøtker, J.P., Rantanen, J., 2018b. Additive manufacturing of prototype elements with process interfaces for continuously operating manufacturing lines. Asian. J. Pharm. Sci 13, 575–583. https://doi.org/10.1016/j.ajps.2018.04.007.

Ho, B.H.K., Chen, C.J., Tan, G.J.S., Yeong, W.Y., Tan, H.K.J., Lim, A.Y.H., Ferenczi, M.A., Mogali, S.R., 2019. Multi-material three dimensional printed models for simulation of bronchoscopy. BMC. Med. Educ 19, 236. https://doi.org/10.1186/s12909-019-1677-9.

Huang, F., Zhou, X., Dai, W., Yu, J., Zhou, Z., Tong, Z., Yu, A., 2022. In Vitro and In Silico Investigations on Drug Delivery in the Mouth-Throat Models with Handihaler. Pharm. Res 39, 3005–3019. https://doi.org/10.1007/s11095-022-03386-9.

Huang, J., Koutsos, V., Radacsi, N., 2020. Low-cost FDM 3D-printed modular electrospray/electrospinning setup for biomedical applications. In: 3D Print Med 6. https://doi.org/10.1186/s41205-020-00060-x.

Kara, A., Kumar, D., Healy, A.M., Lalatsa, A., Serrano, D.R., 2023. Continuous manufacturing of cocrystals using 3D-printed microfluidic chips coupled with spray coating. Pharmaceuticals 16. https://doi.org/10.3390/ph16081064.

Kaviratna, A., Tian, G., Liu, X., Delvadia, R., Lee, S., Guo, C., 2019. Evaluation of bio-relevant mouth-throat models for characterization of metered dose inhalers. AAPS. PharmSciTech 20, 130. https://doi.org/10.1208/s12249-019-1339-6.

Kramek-Romanowska, K., Stecka, A.M., Zielinski, K., Dorosz, A., Okrzeja, P., Michnikowski, M., Odziomek, M., 2021. Independent Lung Ventilation-Experimental Studies on a 3D Printed Respiratory Tract Model. Materials 14, 5189. https://doi.org/10.3390/ma14185189.

Lee, M., Yoon, K., Cho, B., Kim, S.S., Song, S.Y., Choi, E.K., Ahn, S., Lee, S., Kwak, J., 2019. Comparing phase- and amplitude-gated volumetric modulated arc therapy for stereotactic body radiation therapy using 3D printed lung phantom. J. Appl. Clin. Med. Phys 20, 107–113. https://doi.org/10.1002/acm2.12533.

Li, J., Baxani, D.K., Jamieson, W.D., Xu, W., Rocha, V.G., Barrow, D.A., Castell, O.K., 2020a. Formation of polarized, functional artificial cells from compartmentalized droplet networks and nanomaterials, using one-step, dual-material 3D-printed microfluidics. Adv. Sci. 7. https://doi.org/10.1002/advs.201901719.

Li, Y., Bohr, A., Jensen, H., Rantanen, J., Cornett, C., Beck-Broichsitter, M., Bøtker, J.P., 2020b. Medication Tracking: Design and Fabrication of a Dry Powder Inhaler with Integrated Acoustic Element by 3D Printing. Pharm. Res 37. https://doi.org/10.1007/s11095-020-2755-8.

Lim, S.H., Kathuria, H., Tan, J.J.Y., Kang, L., 2018. 3D printed drug delivery and testing systems — a passing fad or the future? Adv. Drug. Deliv. Rev 132, 139–168. https://doi.org/10.1016/j.addr.2018.05.006.

Lim, S.H., Park, S., Lee, C.C., Ho, P.C.L., Kwok, P.C.L., Kang, L., 2021. A 3D printed human upper respiratory tract model for particulate deposition profiling. Int. J. Pharm 597, 120307. https://doi.org/10.1016/j.ijpharm.2021.120307.

McDonough, J.R., Law, R., Reay, D.A., Groszek, D., Zivkovic, V., 2020. Miniaturisation of the toroidal fluidisation concept using 3D printing. Chem. Eng. Res. Des. 160, 129–140. https://doi.org/10.1016/j.cherd.2020.04.031.

Moraga-Espinoza, D., Warnken, Z.N., Moore, A., Williams, R.O., Smyth, H.D.C., 2018. A modified USP induction port to characterize nasal spray plume geometry and predict turbinate deposition under flow. Int. J. Pharm 548, 305–313. https://doi.org/10.1016/j.ijpharm.2018.06.058.

Niese, S., Breitkreutz, J., Quodbach, J., 2019. Development of a dosing device for individualized dosing of orodispersible warfarin films. Int. J. Pharm 561, 314–323. https://doi.org/10.1016/j.ijpharm.2019.03.019.

Nodilo, L., Ugrina, I., Špoljarić, D., Amidžić Klarić, D., Brala, C., Perkušić, M., Pepić, I., Lovrić, J., Saršon, V., Safundžić Kučuk, M., Zadravec, D., Kalogjera, L., Hafner, A., 2021. A Dry Powder Platform for Nose-to-Brain Delivery of Dexamethasone: Formulation Development and Nasal Deposition Studies. Pharmaceutics 13, 795. https://doi.org/10.3390/pharmaceutics13060795.

FDA, 2022. Overview FDA's Regulatory Framework for 3D Printing Of Medical Devices at the Point of Care Needs More Clarity. https://doi.org/https://www.pewtrusts.org/en/research-and-analysis/issue-briefs/2022/07/fdas-regulatory-framework-for-3d-printing-of-medical-devices-needs-more-clarity.

Parhi, R., 2021. A review of three-dimensional printing for pharmaceutical applications: Quality control, risk assessment and future perspectives. J. Drug. Deliv. Sci. Technol. https://doi.org/10.1016/j.jddst.2021.102571.

Peterman, E.L., Kolewe, E.L., Fromen, C.A., n.d. - Evaluating Regional Pulmonary Deposition using Patient-Specific 3D Printed Lung Models. Doi: 10.3791/61706.

Pozzoli, M., Ong, H.X., Morgan, L., Sukkar, M., Traini, D., Young, P.M., Sonvico, F., 2016. Application of RPMI 2650 nasal cell model to a 3D printed apparatus for the testing of drug deposition and permeation of nasal products. Eur. J. Pharm. Biopharm. 107, 223–233. https://doi.org/10.1016/j.ejpb.2016.07.010.

Ren, W., Murawsky, M., La Count, T., Wanasathop, A., Hao, X., Kelm, G.R., Kozak, D., Qin, B., Li, S.K., 2019. Dissolution Chamber for Small Drug Delivery System in the Periodontal Pocket. AAPS J. 21. https://doi.org/10.1208/s12248-019-0317-y.

Sawant, N., Donovan, M.D., 2018. In Vitro Assessment of Spray Deposition Patterns in a Pediatric (12 Year-Old) Nasal Cavity Model. Pharm. Res 35, 108–112. https://doi.org/10.1007/s11095-018-2385-6.

Senjoti, F.G., Ghori, M.U., Diryak, R., Conway, B.R., Morris, G.A., Smith, A.M., 2020. Rheo-dissolution: A new platform for the simultaneous measurement of rheology and drug release. Carbohydr. Polym 229. https://doi.org/10.1016/j.carbpol.2019.115541.

Sheikh, Z., Granata, A., Zhang, Y., Mahvizani, H.M.G., Silva, D., Young, P.M., Casettari, L., Ong, H.X., Traini, D., 2023. The development of a 3D-printed in vitro integrated oro-pharyngeal air–liquid interface cellular throat model for drug transport. Drug. Deliv. Transl. Res 13, 1405–1419. https://doi.org/10.1007/s13346-023-01302-1.

Sil, B.C., Alvarez, M.P., Zhang, Y., Kung, C.P., Hossain, M., Iliopoulos, F., Luo, L., Crowther, J.M., Moore, D.J., Hadgraft, J., Lane, M.E., Hilton, S.T., 2018. 3D-printed Franz type diffusion cells. Int. J. Cosmet. Sci 40, 604–609. https://doi.org/10.1111/ics.12504.

Sommonte, F., Weaver, E., Mathew, E., Denora, N., Lamprou, D.A., 2022. In-House Innovative "Diamond Shaped" 3D Printed Microfluidic Devices for Lysozyme-Loaded Liposomes. Pharmaceutics 14. https://doi.org/10.3390/pharmaceutics14112484.

Sonnenberg, A.H., Taylor, E., Mondoñedo, J.R., Jawde, S.B., Amin, S.D., Song, J., Grinstaff, M.W., Suki, B., 2021. Breath Hold Facilitates Targeted Deposition of Aerosolized Droplets in a 3D Printed Bifurcating Airway Tree. Ann. Biomed. Eng 49, 812–821. https://doi.org/10.1007/s10439-020-02623-9.

Speer, I., Preis, M., Breitkreutz, J., 2019. Novel Dissolution Method for Oral Film Preparations with Modified Release Properties. AAPS. PharmSciTech 20. https://doi.org/10.1208/s12249-018-1255-1.

Suarato, G., Spanò, R., Bertorelli, R., Diaspro, A., Athanassiou, A., Surdo, S., 2018. 3D-Printed, Pocket-Size Diffusion Cells for Skin Permeation Investigation. MDPI. AG 945. https://doi.org/10.3390/proceedings2130945.

Suwanpitak, K., Lim, L.Y., Singh, I., Sriamornsak, P., Thepsonthi, T., Huanbutta, K., Sangnim, T., 2022. Development of an Add-On Device Using 3D Printing for the Enhancement of Drug Administration Efficiency of Dry Powder Inhalers (Accuhaler). Pharmaceutics 14. https://doi.org/10.3390/pharmaceutics14091922.

Svane, R., Pedersen, T., Hirschberg, C., Rantanen, J., 2021. Rapid Prototyping of Miniaturized Powder Mixing Geometries. J. Pharm. Sci 110, 2625–2628. https://doi.org/10.1016/j.xphs.2021.03.019.

Thomas G. West, T.J.B., 2018. 3D Printing: A Case of ZipDose® Technology – World's First 3D Printing Platform to Obtain FDA Approval for a Pharmaceutical Product. 3D and 4D Printing in Biomedical Applications: Process Engineering and Additive Manufacturing.

Tiboni, M., Curzi, G., Aluigi, A., Casettari, L., 2021a. An easy 3D printing approach to manufacture vertical diffusion cells for in vitro release and permeation studies. J. Drug. Deliv. Sci. Technol 65. https://doi.org/10.1016/j.jddst.2021.102661.

Tiboni, M., Tiboni, M., Pierro, A., Del Papa, M., Sparaventi, S., Cespi, M., Casettari, L., 2021b. Microfluidics for nanomedicines manufacturing: An affordable and low-cost 3D printing approach. Int. J. Pharm 599. https://doi.org/10.1016/j.ijpharm.2021.120464.

Van Strien, J., Shrestha, K., Gabriel, S., Lappas, P., Fletcher, D.F., Singh, N., Inthavong, K., 2021. Pressure distribution and flow dynamics in a nasal airway using a scale resolving simulation. Physics. of. Fluids 33, 11907. https://doi.org/10.1063/5.0036095.

Wanasathop, A., Murawsky, M., Li, S.K., 2022. Modification of small dissolution chamber system for long-acting periodontal drug product evaluation. Int. J. Pharm 618. https://doi.org/10.1016/j.ijpharm.2022.121646.

Warnken, Z.N., Smyth, H.D.C., Davis, D.A., Weitman, S., Kuhn, J.G., Williams III, R.O., 2018. Personalized Medicine in Nasal Delivery: The Use of Patient-Specific Administration Parameters To Improve Nasal Drug Targeting Using 3D-Printed Nasal Replica Casts. Mol. Pharm 15, 1392–1402. https://doi.org/10.1021/acs.molpharmaceut.7b00702.

Weaver, E., O'Hagan, C., Lamprou, D.A., 2022. The sustainability of emerging technologies for use in pharmaceutical manufacturing. Expert. Opin. Drug. Deliv. https://doi.org/10.1080/17425247.2022.2093857.

Wilkins, J.V., Golshahi, L., Rahman, N., Li, L., 2021. Evaluation of Intranasal Vaccine Delivery Using Anatomical Replicas of Infant Nasal Airways. Pharm. Res 38, 141–153. https://doi.org/10.1007/s11095-020-02976-9.

Wong, C.Y.J., Cuendet, M., Spaleniak, W., Gholizadeh, H., Marasini, N., Ong, H.X., Traini, D., 2022. Validation of a cell integrated next-generation impactor to assess in vitro drug transport of physiologically relevant aerosolised particles. Int. J. Pharm 624. https://doi.org/10.1016/j.ijpharm.2022.122024.

Wu, H., Wang, M., Wang, J., An, Y., Wang, H., Huang, Y., 2019. Direct visualizations of air flow in the human upper airway using in-vitro models. Sci. China. Life. Sci 62, 235–243. https://doi.org/10.1007/s11427-018-9373-y.

Xu, J., Sullivan, C., Ong, H.X., Williamson, J.P., Traini, D., Hersch, N., Byrom, M., Young, P.M., 2021. Using individualized three-dimensional printed airway models to guide airway stent implantation. Interact. Cardiovasc. Thorac. Surg 31, 900–903. https://doi.org/10.1093/icvts/ivaa206.

Yang, Y., Li, L., Pan, Y., Sun, Z., 2017. Energy Consumption Modeling of Stereolithography-Based Additive Manufacturing Toward Environmental Sustainability. J. Ind. Ecol 21, S168–S178. https://doi.org/10.1111/jiec.12589.

Ye, Y., Fan, Z., Ma, Y., Zhu, J., 2023. Investigation on the influence of design features on the performance of dry powder inhalers: Spiral channel, mouthpiece dimension, and gas inlet. Int. J. Pharm 642. https://doi.org/10.1016/j.ijpharm.2023.123116.

Yea, J.W., Park, J.W., Kim, S.K., Kim, D.Y., Kim, J.G., Seo, C.Y., Jeong, W.H., Jeong, M. Y., Oh, S.A., 2017. Feasibility of a 3D-printed anthropomorphic patient-specific head phantom for patient-specific quality assurance of intensity-modulated radiotherapy. PLoS. One 12, e0181560–e. https://doi.org/10.1371/journal.pone.0181560.

Zhang, Y., Goh, K.-L., Ling Ng, Y., Chow, Y., Zivkovic, V., 2021a. Design and investigation of a 3D-printed micro-fluidized bed. 5. Doi: 10.3390/chemengineering5030062.

Zhang, Y., Goh, K.L., Ng, Y.L., Chow, Y., Wang, S., Zivkovic, V., 2021b. Process intensification in micro-fluidized bed systems: A review. Chem. Eng. Processing. -. Process. Intensification. https://doi.org/10.1016/j.cep.2021.108397.